DETAILED STUDY OF BIFURCATIONS IN AN
EPIDEMIC MODEL ON A DYNAMIC NETWORK

ANDRÁS SZABÓ, PÉTER L. SIMON AND ISTVAN Z. KISS

Abstract. The bifurcations in a four-variable ODE model of an SIS type epidemic on an adaptive network are studied. The model describes the propagation of the epidemic on a network where links (or edges) of different type (i.e. *SI,II* and *SS*) can be activated or deleted according to a simple rule consisting of random link activation and deletion. In the case when *II* links cannot be neither deleted nor created it is proved that the system can have at most three steady states with the trivial, disease-free steady state being one of them. It is shown that a stable endemic steady state can appear through a transcritical bifurcation, or a stable and an unstable endemic steady state arise as a result of saddle-node bifurcation. Moreover, at the endemic steady state a Hopf bifurcation may occur giving rise to stable oscillation. The bifurcation curves in the parameter space are determined analytically using the parametric representation method. For certain parameter regimes or bifurcation types, analytical results based on the ODE model show good agreement when compared to results based on individual-based network simulations. When agreement between the two modelling approaches holds, the ODE-based model provides a faster and more reliable tool that can be used to explore full spectrum of model behaviour.

1. Introduction

Recently, it has become more and more important to understand the relation between the dynamics on a network and the dynamics of the network [5]. In the case of epidemic propagation on networks it is straightforward to assume that the propagation of the epidemic has an effect on the structure of the network. For example, susceptible individuals try to cut their links in order to minimise their exposure to infection. This leads to a change in network structure which in turn impacts on how the epidemic spreads. This phenomenon can be modeled by using two main approaches: (i) individual based stochastic simulations or micro models and (ii) macro models where variables at the population level are given in terms of a system of ordinary differential equations. These types of models can have several parameters and, especially in the latter case, the behaviour of the system can be rigorously investigated via bifurcation analysis techniques. The aim this paper is twofold. First, we revisit the formulation of a dynamic network model which is coupled with a simple epidemic dynamics and,

second, we use bifurcation analysis to analyse the full spectrum of model behaviour. We use our results to highlight the importance of coupled models in understanding real world processes.

Over the last few years several models have been proposed where both the dynamics of the network and on the network are considered [5]. For example, Saramäki and Kaski [10] proposed an SIR model where in a cycle graph long-range links are introduced randomly. These links account for occasional, far away infection, i.e. an infected node, at some rate, can infect nodes that are not immediate local neighbours. They formulate a simple ODE model that is similar to pairwise models [7] and use this to derive analytic results for disease transmission threshold and to validate simulation results. Gross et al. [4] proposed a model where (SI) links are cut at a certain rate with susceptible nodes immediately re-wiring to other susceptible nodes chosen at random from the entire population. Again, a simple pairwise type model was used to derive an ODE that describes the interaction of network and disease dynamics. Shaw and Schwartz generalised this investigation to an SIRS type model [11]. Risau-Gusman and Zanette [9] considered the case when the susceptible node from an (SI) pair re-wires to a node chosen at random from the entire network regardless of its state, with the infected node in an (SI) pair being able to perform the same re-wiring.

Recently, we have proposed a model in which the immediate re-wiring is not assumed and all type of contacts (i.e. SS, SI and II) can be activated or deleted at a certain rate. The first aim of that paper was to investigate the impact of these simple network dynamics on the structure of the network when node dynamic was absent and when the nodes were static but labeled. Then the dynamic network was coupled with SIS node dynamics and a pairwise and simulation model were used to investigate and characterise the full spectrum of behaviour. In that paper, the analysis mainly focused on the agreement between simulation and pairwise models with the detailed analytical study of bifurcations postponed to the present paper. The proposed model has 8 parameters and hence a numerical bifurcation study is difficult to perform in order to reveal the full spectrum of behaviour. Thus main aim of this paper is the detailed analytical study of bifurcations that occur in the system and to identify regions where the different behaviours can be observed. To achieve this we apply the parametric representation method which is a useful tool that can be used to find the bifurcation curves analytically and has already been used successfully to analyse different systems [1, 8, 12].

In the paper the following pair approximation model for an SIS epidemic propagating on a dynamically changing graph with N nodes is considered,

$$[\dot{I}] = \tau[SI] - \gamma[I], \tag{1}$$

$$[\dot{SI}] = \gamma([II] - [SI]) + \tau([SSI] - [ISI] - [SI])$$
$$- \omega_{SI}[SI] + \alpha_{SI}([S][I] - [SI]), \tag{2}$$

$$[\dot{II}] = -2\gamma[II] + 2\tau([ISI] + [SI]) - \omega_{II}[II] + \alpha_{II}([I]([I] - 1) - [II]), \tag{3}$$

$$[\dot{SS}] = 2\gamma[SI] - 2\tau[SSI] - \omega_{SS}[SS] + \alpha_{SS}([S]([S] - 1) - [SS]). \tag{4}$$

Here $[I](t)$ is the expected number of infected nodes in the graph at time t and

$[SI](t)$, $[II](t)$, $[SS](t)$ denote the expected number of SI, II and SS edges at time t. Similar notation is used for the triples SSI and ISI. The parameters of the epidemic propagation are τ, the infection rate and γ the recovery rate. The parameters of the dynamic of the graph are $\alpha_{SI}, \alpha_{II}, \alpha_{SS}$, the rates of activation of the corresponding links, and $\omega_{SI}, \omega_{II}, \omega_{SS}$ the rates of deletion of the corresponding links. The deletion of links is simply assumed to be proportional to the number of existing links, for example, the deletion of SI edges is given by the term $\omega_{SI}[SI]$. Similarly, the activation of links is proportional to the number of potential links that are not yet connected, for example, the activation of SI edges is described by the term $\alpha_{SI}([S][I] - [SI])$.

The following simple closures are used for the triples,

$$[SSI] = \frac{n-1}{n}\frac{[SS][SI]}{[S]}, \qquad [ISI] = \frac{n-1}{n}\frac{[IS][SI]}{[S]},$$

where n is the average degree of the nodes. This type of closure is widely used for homogeneous random graphs [6, 7] with no clustering (i.e. neighbours of a node are not or very unlikely to be neighbours of each other) and also for unclustered random graphs with close to Poisson degree distribution [14]. In this case, the closure relations including the clustering coefficient do not seem to perform better when compared to the simpler closure. This is simply explained by the fact that for large parameter regions the dynamic graph becomes densely connected. This correlates with high clustering, but with its effect being significantly weakened by the high link density. Hence, even when clustering is high, the mean-field limit gives a good approximation like in the case of a fully connected graph. Namely, for a complete graph the clustering coefficient is equal to 1, and despite of this, the above closure relations without clustering coefficient perform very well. Due to the dynamic nature of the network, the average degree of the nodes, where degree is simply the number of links or edges a node has, is a variable itself and changes with time as $n(t) = (2[SI](t) + [II](t) + [SS](t))/N$. Hence, the analysis above performed for a fixed n serves only as an indicator of possible system behaviours but can give good results if n is a slow variable where for example the network dynamics is much slower compared to the epidemic or if n does not vary considerably. We also note that n only enters via the $(n-1)/n$ term which for realistic networks that are well connected is close to one. In [15] we showed that for wide parameter regions the simulation model justifies the use of the above closure and explained why for some parameters the agreement breaks down. We briefly revisit this aspect in the Discussion section and we present further evidence of good agreement between the ODE model and simulation.

In order to make the notations simpler the following new variables will be used,

$$x = [I], \quad y = [SI], \quad z = [II], \quad u = [SS].$$

Using these notations and the above closure relations our system (1)-(4) takes the form

$$\dot{x} = \tau y - \gamma x, \tag{5}$$

$$\dot{y} = \gamma(z - y) + \tau\frac{n-1}{n}\frac{y(u-y)}{N-x} - \tau y - \omega_{SI}y + \alpha_{SI}\big((N-x)x - y\big), \tag{6}$$

$$\dot{z} = -2\gamma z + 2\tau\left(\frac{n-1}{n}\frac{y^2}{N-x} + y\right) - \omega_{II}z + \alpha_{II}\big(x(x-1) - z\big), \tag{7}$$

$$\dot{u} = 2\gamma y - 2\tau\frac{n-1}{n}\frac{uy}{N-x} - \omega_{SS}u + \alpha_{SS}((N-x)(N-x-1) - u). \tag{8}$$

We note that the new variables are not rescaled because of two reasons. On one hand, the theoretical results are easier to compare to simulations when the same parameters are used, this is why τ and γ are not scaled. On the other hand, the often used normalization by introducing $[I]/N$ as a new variable requires scaling of order N^2 for the pairs, which is useful in the case of a static graph, however, in the case of a dynamically changing graph the number of pairs can be also of order N.

The aim of the paper is to determine the number of stationary states and their local bifurcations analytically. It will be shown that a relatively rich bifurcation behaviour can be identified with respect to other epidemic adaptive network models. There are three types of bifurcations. First, a transcritical bifurcation where the disease-free steady state loses stability giving rise to a stable endemic equilibrium. Second, a saddle-node bifurcation which gives rise to the co-existence of two stable equilibria (one being disease-free and the other endemic) with an unstable equilibrium, and finally, a Hopf bifurcation, where the stable endemic equilibrium looses its stability and gives rise to a stable limit cycle.

The paper is structured as follows. In Section 2 we show how the algebraic system determining the steady states can be reduced to a single equation, then the saddle-node bifurcation curve is calculated by using the parametric representation method [12], and the exact number of steady states for different domains of the parameter space is determined. In Section 3 the transcritical bifurcation of the trivial steady state is determined analytically, and a semi-analytic way of finding the Hopf bifurcation curve in a plane of two parameters is shown.

2. Number of steady states

The steady states are determined by the system of four equations obtained from (5)-(8) by putting zeros to the left hand sides. This four variable system can easily be reduced to a single (higher degree) equation for the variable x. This reduction will be shown in the first Subsection. Then in the next two Subsections the number of solutions of this reduced equation will be studied.

2.1. Reduction to a single equation

Let us consider system (5)-(8) with zeros in the left hand sides. From the first equation y can be expressed in terms of x, then from the third equation z can be expressed in terms of x, and finally, from the fourth equation u can be expressed in terms of x as follows:

$$y = \frac{\gamma}{\tau}x, \quad z = xf_z(x), \quad u = (N-x)f_u(x), \tag{9}$$

where

$$f_z(x) = \frac{2\gamma\left(\frac{n-1}{n}\frac{\gamma x}{\tau(N-x)}+1\right)+\alpha_{II}(x-1)}{2\gamma+\omega_{II}+\alpha_{II}},$$

$$f_u(x) = \frac{2\gamma^2 x/\tau + \alpha_{SS}(N-x)(N-x-1)}{2\gamma\frac{n-1}{n}x+(\omega_{SS}+\alpha_{SS})(N-x)}. \tag{10}$$

Substituting these expressions of y, z and u into the second equation we get the following equation for x

$$\gamma x\left(f_z(x)-\frac{\gamma}{\tau}\right)+\gamma x\frac{n-1}{n}\left(f_u(x)-\frac{\gamma x}{\tau(N-x)}\right)-\gamma x-\omega_{SI}\frac{\gamma}{\tau}x$$
$$+\alpha_{SI}\left((N-x)x-\frac{\gamma}{\tau}x\right)=0. \tag{11}$$

One can see that $x = 0$ is a solution, hence there is a trivial (disease-free) equilibrium corresponding to

$$x=0, \quad y=0, \quad z=0, \quad u=u^*=\frac{N(N-1)\alpha_{SS}}{\omega_{SS}+\alpha_{SS}}. \tag{12}$$

Besides this trivial solution there can be endemic equilibria the x coordinate of which are given by (11), that is a fourth degree equation after multiplying by the product of the denominators. One can observe that in the case $\alpha_{II}=\omega_{II}=0$ the terms containing $N-x$ in the denominator cancel, and hence the equation only needs to be multiplied with the (linear) denominator of $f_u(x)$. Therefore the resulting equation will be of third degree, and analytically, this is more tractable. This assumption is also supported from the biological point of view, since neither the activation nor the deletion of $[II]$ are likely to happen in a real situation. Our analytical calculations are carried out under the assumption of $\alpha_{II}=\omega_{II}=0$, and we will show numerical evidence that, for non-zero values of these parameters the qualitative behaviour of the bifurcation curves do not change.

In the case $\alpha_{II}=0=\omega_{II}$ the function $f_z(x)$ takes a much simpler form:

$$f_z(x)=\frac{n-1}{n}\frac{\gamma x}{\tau(N-x)}+1.$$

Then (11) simplifies to

$$-\gamma^2 x+\gamma x\frac{n-1}{n}\tau f_u(x)-\omega_{SI}\gamma x+\alpha_{SI}(\tau(N-x)x-\gamma x)=0, \tag{13}$$

which is a third degree equation once it is multiplied by the denominator of $f_u(x)$ and by τ.

Summarising the above, we have shown the following concerning the equilibria.

PROPOSITION 1. *In the case $\alpha_{II}=0=\omega_{II}$ system* (5)-(8) *has at most three steady states. One of them is the trivial steady state given by* (12). *The point (x,y,z,u) is a non-trivial steady state if and only if x is a non-zero solution of* (13) *and y,z,u are given by* (9).

2.2. The discriminant (saddle-node or fold bifurcation) curve

Now our aim is to determine the exact number of solutions of equation (13) for all possible parameter values. Since the two most important parameters τ and ω_{SI} (that are also used in [4]) are involved linearly in the equation the parametric representation method (PRM) [12] can be used to investigate the number of solutions of the third degree equation (13). In order to use this method, equation (13), after dividing by x, can be written in the form

$$f_0(x) + \tau f_1(x) + \omega_{SI} f_2(x) = 0, \tag{14}$$

where

$$f_0(x) = -\gamma\big(2\alpha_{SI}\gamma qx + (\gamma + \alpha_{SI})\rho_{SS}(N-x)\big), \tag{15}$$

$$f_1(x) = (N-x)\big(\alpha_{SS}\gamma q(N-x-1) + \alpha_{SI}(2\gamma qx + \rho_{SS}(N-x))\big), \tag{16}$$

$$f_2(x) = -\gamma\big(2\gamma qx + \rho_{SS}(N-x)\big), \tag{17}$$

$q = \frac{n-1}{n}$ and $\rho_{SS} = \omega_{SS} + \alpha_{SS}$. Our first aim is to divide the (τ, ω_{SI}) parameter plane according to the number of steady states, i.e. the number of solutions of (14). The discriminant curve, that is also called saddle-node or fold bifurcation curve divides the parameter plane according to the number of solutions. We will refer to this curve shortly as D-curve, it will be defined in the next Subsection.

2.2.1. Determination of the D-curve

According to the Implicit Function Theorem the number of solutions of (14) can change when the derivative of the left hand side is also zero, that is

$$f_0'(x) + \tau f_1'(x) + \omega_{SI} f_2'(x) = 0. \tag{18}$$

Equations (14) and (18) determine the singularity set or the so-called discriminant curve in the (τ, ω_{SI}) parameter plane as follows

$$S = \{(\tau, \omega_{SI}) \in \mathbb{R}^2 \ : \ \exists x \in \mathbb{R}, \text{ such that (14), (18) hold}\}.$$

This set, along which the number of solutions can change, is usually determined by eliminating x from system (14), (18). This way an expression can be derived relating τ to ω_{SI}. This expression used to be quite complicated, hence it is not easy to plot the singularity set numerically or determine its properties analytically. The essence of the parametric representation method is to exploit the fact that system (14), (18) contains the parameters τ and ω_{SI} linearly, hence these can be expressed in terms of x. Thus the singularity set can be given as a curve parametrised by x, this curve will be referred to as D-curve or discriminant curve. The point of the D-curve corresponding to x will be denoted by $D(x) = (D_1(x), D_2(x))$, where $D_1(x)$ yields τ and $D_2(x)$ yields ω_{SI}. Thus solving the linear system (14), (18) for τ and ω_{SI} we get

$$D_1(x) = \frac{f_0'(x)f_2(x) - f_0(x)f_2'(x)}{f_1(x)f_2'(x) - f_1'(x)f_2(x)}, \quad D_2(x) = \frac{f_0(x)f_1'(x) - f_0'(x)f_1(x)}{f_1(x)f_2'(x) - f_1'(x)f_2(x)}. \tag{19}$$

It is straightforward to express these functions in terms of the original parameters since f_0, f_2 are linear and f_1 is quadratic function of x. After some algebra we get

$$f_0'(x)f_2(x) - f_0(x)f_2'(x) = -2N\gamma^4 q\rho_{SS}, \tag{20}$$

$$f_1(x)f_2'(x) - f_1'(x)f_2(x) = -2N\gamma^2 q((N-1)q\gamma\alpha_{SS} + N\alpha_{SI}\rho_{SS})$$
$$+(\gamma q(\alpha_{SS} - 2\alpha_{SI}) + \alpha_{SI}\rho_{SS})(2\gamma^2 qx^2 - \gamma\rho_{SS}(N-x)^2), \tag{21}$$

$$f_0(x)f_1'(x) - f_0'(x)f_1(x) = 2N\gamma^2\alpha_{SI}q((N-1)q\gamma\alpha_{SS} + N\alpha_{SI}\rho_{SS})$$
$$-(\gamma q(\alpha_{SS} - 2\alpha_{SI}) + \alpha_{SI}\rho_{SS})(2\gamma^2\alpha_{SI}qx^2 - \gamma(\gamma + \alpha_{SI})\rho_{SS}(N-x)^2). \tag{22}$$

Thus for given values of the parameters $N, n, \alpha_{SI}, \alpha_{SS}, \omega_{SS}$ the D-curve can be easily plotted as a parametric curve in the (τ, ω_{SI}) parameter plane, the parameter x runs in the interval $[0, N]$. The typical shape of the curve is shown in Figure 1.

2.2.2. Main results of the PRM concerning the D-curve

Now we explain how can the number of steady states be determined by using the parametric representation method. The first advantage of the PRM, that was exploited in the previous Subsection, is that the singularity set can easily be determined. The second one is the so-called tangential property [12, 13] that says the following.

LEMMA 1. (Tangential property) *For a given parameter pair (τ, ω_{SI}) the number of solutions of equation (14) is equal to the number of tangents that can be drawn to the D-curve from the given (τ, ω_{SI}) parameter pair. The values of the solutions can be read as the value x of the tangent point on the D-curve.*

Moreover, the so-called convexity property helps to count the number of tangents easily [12, 13].

LEMMA 2. (Convexity property) *The D-curve consists of convex arcs, meaning that every arc lies on one side of its tangents. These arcs join at cusp points of the D-curve. There is a cusp point at x_0, if the function $f_0''(x) + f_1''(x)D_1(x) + f_2''(x)D_2(x)$ changes sign at $x = x_0$.*

The use of the convexity property is based on the fact that to each convex arc there can be drawn at most two tangents. The exact number of tangents depends on the position of the point as it is shown in Figure 2.

Thus in order to use the PRM to determine the exact number of steady states we need the following characteristic properties of the D-curve, that help to determine the exact number of tangents from different points: the cusp points, the tangents at the endpoints and the position of the curve. These characteristic properties will be studied in the next Subsection.

2.2.3. Characterisation of the D-curve

In our case the functions f_0, f_2 are linear and f_1 is quadratic, hence it can be shown that the D-curve has no cusp point, which yields that it consists of a single convex arc (as it also can be seen in Figure 1).

Let us now investigate the tangent lines belonging to the endpoints $x = 0$ and $x = N$. According to the tangential property, the equation of these lines are $f_0(0) + \tau f_1(0) + \omega_{SI} f_2(0) = 0$ and $f_0(N) + \tau f_1(N) + \omega_{SI} f_2(N) = 0$. The second line is easier to plot, since $f_1(N) = 0$, hence its normal vector is vertical. This line contains the point $D(N)$, which is below the $\omega_{SI} = 0$ coordinate axis, hence this line, as being horizontal, does not enter the positive quadrant of the (τ, ω_{SI}) parameter plane. Let us consider now the other tangent line $f_0(0) + \tau f_1(0) + \omega_{SI} f_2(0) = 0$. It is easy to see that $f_2(0) < 0 < f_1(0)$, hence this line enters the positive quadrant. Substituting $x = 0$ into (15)-(17) we get for the equation of this line

$$\gamma(\gamma + \alpha_{SI})\rho_{SS} - \tau((N-1)\alpha_{SS}\gamma q + N\alpha_{SI}\rho_{SS}) + \omega_{SI}\gamma\rho_{SS} = 0. \tag{23}$$

Thus the D-curve and its tangents at the endpoints can divide the positive quadrant of the (τ, ω_{SI}) parameter plane into three regions as it is shown in Figure 3.

The convexity of the D-curve and the position of its tangents at the endpoints do not depend on the value of the parameters in the system. Hence for all values of the parameters we can have the above regions according to the number of tangents. The only thing that the parameter values can change is the position of the endpoint $D(0)$. This may be pushed down below the $\omega_{SI} = 0$ coordinate axis, and then region 3 disappears. Let us now investigate the position of the D-curve in detail. It is determined by the signs of the numerators and denominators in (19). The numerator in D_1 is negative. The signs of the other two expressions are given in the following Proposition.

PROPOSITION 2. 1. *The functions $f_1 f_2' - f_1' f_2$ and $f_0 f_1' - f_0' f_1$ are monotone in the interval $[0, N]$.*

2. *For any values of the parameters we have $f_1(0)f_2'(0) - f_1'(0)f_2(0) < 0$ and*

$$f_1(N)f_2'(N) - f_1'(N)f_2(N) = 2\gamma^3 q^2 N(\alpha_{SS} - 2N\alpha_{SI})$$
$$= -\frac{1}{\alpha_{SI}}(f_0(N)f_1'(N) - f_0'(N)f_1(N)).$$

3. *Inequality $f_0(0)f_1'(0) - f_0'(0)f_1(0) < 0$ holds if and only if the following condition is satisfied*

$$2q^2\alpha_{SI}\alpha_{SS}(1 - \frac{1}{N}) + (q\alpha_{SS} + \frac{\alpha_{SI}}{\gamma}\rho_{SS})(1 + \frac{\alpha_{SI}}{\gamma})\rho_{SS} < 2q\alpha_{SI}\rho_{SS}. \tag{24}$$

Proof. 1. We have $(f_1 f_2' - f_1' f_2)' = f_1 f_2'' - f_1'' f_2 = -f_1'' f_2$ since $f_2'' = 0$ (f_2 is linear). The function f_1 is quadratic, hence the derivative $(f_1 f_2' - f_1' f_2)'$ is a linear function, the sign of which is determined by the sign of f_2. It is easy to see that f_2

does not change sign in the interval $[0,N]$, therefore the derivative $(f_1 f_2' - f_1' f_2)'$ also has constant sign in this interval. The proof of the monotonicity of $f_0 f_1' - f_0' f_1$ is similar.

The statements in 2 and 3 can be proved by straightforward calculations using (21)-(22). $\square$

According to the Proposition both the numerator and denominator in $D_1(0)$ are negative, hence $D_1(x) > 0$ when x is small. For the function D_2 we have $D_2(N) = -\alpha_{SI}$, that is $D_2(x) < 0$ when x is close to N. The D-curve enters the positive quadrant if and only if the numerator of $D_2(0)$ is negative, that is when (24) holds. Otherwise, the D-curve is completely below the $\omega_{SI} = 0$ coordinate axis, which means that region 3 does not exist. Summarising, we can say that the position of the D-curve is determined by condition (24).

2.2.4. Determination of the number of steady states using the D-curve

Let us consider now the D-curve as it is shown in Figure 3. From the points in region 1 there cannot be drawn tangents to the given arc (belonging to $x \in [0,N]$) of the D-curve. Hence, if the pair (τ, ω_{SI}) is in this region then equation (14) has no solution in $[0,N]$. Therefore equation (13) has only the trivial solution $x = 0$, i.e. there is only the trivial disease-free steady state. From the points in region 2 there can be drawn one tangent to the given arc (belonging to $x \in [0,N]$) of the D-curve (see Figure 2). Hence, if the pair (τ, ω_{SI}) is in this region then equation (14) has one solution in $[0,N]$. Therefore equation (13) has the trivial solution $x = 0$ and another solution $x \in (0,N]$, i.e. there are two steady states. From the points in region 3 there can be drawn two tangents to the given arc (belonging to $x \in [0,N]$) of the D-curve (see Figure 2). Hence, if the pair (τ, ω_{SI}) is in this region then equation (14) has two solutions in $[0,N]$. Therefore equation (13) has the trivial solution $x = 0$ and two other solutions in $(0,N]$, i.e. there are three steady states. As it was mentioned earlier, region 3 can disappear if condition (24) does not hold. Hence our results concerning the number of steady states can be summarised as follows.

THEOREM 1. *Let us assume* $\alpha_{II} = 0 = \omega_{II}$ *and consider the line given in* (23) *and the D-curve, given by* (19)*. According to the position of the D-curve there are the following two cases.*

• *If the inequality* (24) *does not hold, then the D-curve is outside the positive quadrant and the line given in* (23) *divides the* (τ, ω_{SI}) *parameter plane into two regions. If the parameter pair* (τ, ω_{SI}) *is in the left region, then there is only the trivial steady state given in* (12)*. If the parameter pair* (τ, ω_{SI}) *is in the right region then there are two steady states (one of them is the trivial steady state).*

• *If the inequality* (24) *holds, then the D-curve and the line given in* (23) *divide the* (τ, ω_{SI}) *parameter plane into three regions. If the parameter pair* (τ, ω_{SI}) *is in the right region then there are two steady states (one of them is the trivial steady state). If the parameter pair* (τ, ω_{SI}) *is in the left region above the D-curve, then there is only*

the trivial steady state given in (12). If the parameter pair (τ, ω_{SI}) is in the left region below the D-curve, then there are three steady states (one of them is the trivial steady state).

In the case when α_{II} and ω_{II} are non-zero then the D-curve can be given similarly, however, formulas become more complicated hence the analytic characterisation is not available. Our numerical investigations show that there are the above two cases also for non-zero values of α_{II} and ω_{II}. In Figure 4 the second case is shown, when the D-curve and its tangent at the end point divide the parameter plane into three regions according to the number of steady states.

3. Bifurcations

In this Section the local bifurcations of the steady states are investigated in the case $\alpha_{II} = 0 = \omega_{II}$. Hence we will need the linearisation at the equilibria. The Jacobian takes the form

$$J = \begin{pmatrix} -\gamma & \tau & 0 & 0 \\ J_{yx} & J_{yy} & \gamma & J_{yu} \\ J_{zx} & J_{zy} & -2\gamma & 0 \\ J_{ux} & J_{uy} & 0 & J_{uu} \end{pmatrix}, \tag{25}$$

where

$$J_{yx} = \tau q y \frac{u-y}{(N-x)^2} + \alpha_{SI}(N-2x),$$

$$J_{yy} = -\gamma + \tau q \frac{u-2y}{N-x} - \tau - \omega_{SI} - \alpha_{SI}, \quad J_{yu} = \frac{\tau q y}{N-x},$$

$$J_{zx} = 2\tau q \frac{y^2}{(N-x)^2}, \quad J_{zy} = 4\tau q \frac{y}{N-x} + 2\tau,$$

$$J_{ux} = -2\frac{\tau q u y}{(N-x)^2} + \alpha_{SS}(1 - 2N + 2x),$$

$$J_{uy} = 2\gamma - 2\frac{\tau q u}{N-x}, \quad J_{uu} = -2\frac{\tau q y}{N-x} - \rho_{SS}.$$

For a given steady state the eigenvalues of matrix J have to be investigated. When $x = 0$, that is for the disease-free steady state, the spectrum of J can be investigated analytically. This will be done in Subsection 3.1, where it will be shown that the disease-free steady state can undergo only a transcritical bifurcation. For the endemic steady states the spectrum of the Jacobian can only be investigated numerically. This will be studied in in Subsection 3.2, where it will be shown that Hopf-bifurcation may occur and the Hopf-bifurcation curve will be determined numerically.

3.1. Transcritical bifurcation

Let us substitute now the coordinates of the disease-free steady state (given by (12)) into the Jacobian matrix J. Then the only non-zero entry in the last coloumn will

be the lower most one $-\rho_{SS}$. Hence this is a negative eigenvalue of the matrix and remaining three eigenvalues are the same as those of the upper-left 3×3 matrix given as

$$A = \begin{pmatrix} -\gamma & \tau & 0 \\ N\alpha_{SI} & A_{yy} & \gamma \\ 0 & 2\tau & -2\gamma \end{pmatrix}, \tag{26}$$

where

$$A_{yy} = -\gamma + \tau q \frac{(N-1)\alpha_{SS}}{\rho_{SS}} - \tau - \omega_{SI} - \alpha_{SI}.$$

The characteristic polynomial of this matrix is

$$\lambda^3 - \lambda^2 \mathrm{Tr} A + \lambda (A_{11} + A_{22} + A_{33}) - \det A,$$

where A_{ii} is the sub-determinant corresponding to the element a_{ii}. The coefficients can be expressed in terms of the parameters as

$$\mathrm{Tr} A = -4\gamma + \tau q \frac{(N-1)\alpha_{SS}}{\rho_{SS}} - \tau - \omega_{SI} - \alpha_{SI},$$

$$A_{11} + A_{22} + A_{33} = -3\gamma (\tau q \frac{(N-1)\alpha_{SS}}{\rho_{SS}} - \omega_{SI} - \alpha_{SI}) - \tau N\alpha_{SI} + \tau\gamma + 5\gamma^2,$$

$$\det A = 2\gamma^2 (-\gamma + \tau q \frac{(N-1)\alpha_{SS}}{\rho_{SS}} - \omega_{SI} - \alpha_{SI}) + 2\tau\gamma N\alpha_{SI}.$$

According to the Routh-Hurwitz criterion all the roots of the characteristic polynomial have negative real part, i.e. the steady state is asymptotically stable, if and only if the following three conditions hold

$$-\mathrm{Tr} A > 0, \quad -(A_{11} + A_{22} + A_{33})\mathrm{Tr} A > -\det A, \quad -\det A > 0.$$

Now we will prove that these three conditions are equivalent to the last one, $\det A < 0$, when $\tau > 0$. In order to do so we write the above three Routh-Hurwitz conditions in terms of the parameters:

$$c_1 + \omega_{SI} - a_1\tau > 0, \tag{27}$$

$$3(c_1 + \omega_{SI} - a_1\tau)(c_2 + \omega_{SI} - a_2\tau) > 2\gamma(c_3 + \omega_{SI} - a_3\tau), \tag{28}$$

$$c_3 + \omega_{SI} - a_3\tau > 0, \tag{29}$$

where

$$a_1 = r - 1, \quad a_2 = r + \frac{N\alpha_{SI} - \gamma}{3\gamma}, \quad a_3 = r + \frac{N\alpha_{SI}}{\gamma}, \quad r = q\frac{(N-1)\alpha_{SS}}{\rho_{SS}},$$

$$c_1 = \alpha_{SI} + 4\gamma, \quad c_2 = \alpha_{SI} + \frac{5}{3}\gamma, \quad c_3 = \alpha_{SI} + \gamma.$$

PROPOSITION 3. *If $\tau > 0$, then condition* (29) *implies conditions* (27) *and* (28).

Proof. The proof is based on the following simple inequalities:

$$a_1 < a_2 < a_3, \qquad c_3 < c_2 < c_1.$$

Using these inequalities we simply get

$$c_1 + \omega_{SI} - a_1\tau > c_3 + \omega_{SI} - a_3\tau > 0,$$

that is (29) implies (27).

Using that $c_1 = c_3 + 3\gamma$ we get

$$c_1 + \omega_{SI} - a_1\tau > c_1 - c_3 + c_3 + \omega_{SI} - a_3\tau > 3\gamma.$$

Moreover, we have $c_2 + \omega_{SI} - a_2\tau > c_3 + \omega_{SI} - a_3\tau > 0$. Hence

$$3(c_1 + \omega_{SI} - a_1\tau)(c_2 + \omega_{SI} - a_2\tau) > 9\gamma(c_3 + \omega_{SI} - a_3\tau)$$
$$> 2\gamma(c_3 + \omega_{SI} - a_3\tau),$$

that is (29) implies (28). □

Thus we have proved the following Theorem.

THEOREM 2. *The disease-free steady state, given by* (12)*, is asymptotically stable if and only if* (29) *is satisfied, that is when*

$$\omega_{SI} > \tau\left(q(N-1)\frac{\alpha_{SS}}{\rho_{SS}} + N\frac{\alpha_{SI}}{\gamma}\right) - \gamma - \alpha_{SI}$$

holds.

It is important to note that the border line of the stability, given in this Theorem, is the same as the tangent line of the D-curve at the point $D(0)$ given in (23). Hence in the domain on the left hand side of this line the trivial steady state is stable and there is no endemic steady state (in fact, this steady state has negative coordinates), while in the right hand side of this line the trivial steady state is unstable and there is (at least one) endemic steady state. This proves the following statement.

COROLLARY 1. *In the* (τ, ω_{SI}) *parameter plane transcritical bifurcation occurs along the line given by* (23).

3.2. Hopf bifurcation

In this Subsection our aim is to investigate the Hopf-bifurcation curve in the (τ, ω_{SI}) parameter plane. A (τ, ω_{SI}) parameter pair is said to be on this curve, if there exists a steady state at which the Jacobian (25) has a pair of pure imaginary eigenvalues. We note that this is only a necessary condition of the Hopf-bifurcation, however, the calculation of the Liapunov-number after center manifold reduction would be too complicated analytically, hence instead we will simply solve the differential equations numerically to decide whether the Hopf-bifurcation is subcritical or supercritical.

In order to give a condition for the existence of pure imaginary eigenvalues let us introduce the characteristic polynomial of (25) in the form

$$\lambda^4 - b_3\lambda^3 + b_2\lambda^2 - b_1\lambda + b_0.$$

We note that $b_3 = \mathrm{Tr}J$, $b_0 = \det J$ and b_1, b_2 can be given as the sum of some subdeterminants of J, the concrete form of which is not important at this moment. In [3] a general formula is given for an $n \times n$ matrix to have purely imaginary eigenvalues. In the case of 4×4 matrices the necessary and sufficient condition for the existence of pure imaginary eigenvalues is

$$b_0 b_3^2 = b_1(b_2 b_3 - b_1) \quad \text{and} \quad \mathrm{sign} b_1 = \mathrm{sign} b_3, \tag{30}$$

see [8]. Thus the Hopf-bifurcation set can be defined as

$$H = \{(\tau, \omega_{SI}) \in \mathbb{R}^2 \; : \; \exists x \in \mathbb{R} \text{ such that (14), (30) hold}\}.$$

This set can also be given as a curve in the (τ, ω_{SI}) parameter plane, however, equation (30) is not linear in the parameters τ and ω_{SI}, hence system (14), (30) cannot be easily solved for τ and ω_{SI}. Nevertheless, we want to express H as a curve parametrised by x in the (τ, ω_{SI}) parameter plane. We have seen in the previous Section that once the x coordinate of the steady state is given, then the other coordinates are determined by (9). Moreover, according to the Tangential property (Lemma 1), if the x coordinate of the steady state is given, then the parameter pair (τ, ω_{SI}) lies on the tangent line of the D-curve drawn at the point $D(x)$, see the insert in Figure 5. Therefore we will determine the points of H in the following way. For a given x we introduce a distance parameter d along the tangent line of the D-curve at $D(x)$, the equation of which is (14). From this equation we determine the τ and ω_{SI} value along the tangent, which determines a point being in distance d from the tangent point $D(x)$. The value of y, z and u are given by (9). Hence in the Jacobian J everything is expressed in terms of x and d. Hence for a given x the coefficients b_i of the characteristic polynomial are functions of d. Thus in order to find the Hopf bifurcation points along the tangent line, we have to solve the first equation in (30) for d. Our numerical experiments show that there are two x values: x_1 and x_2, such that for $x \in (x_1, x_2)$ there two values of d, denoted by $d^{H_1}(x)$ and $d^{H_2}(x)$, that are solutions of the first equation in (30). These are shown in Figure 5. If x is outside this interval, then the first equation in (30) does not have a solution for d. The $d^{H_1}(x)$ and $d^{H_2}(x)$ values determine the value of τ and ω_{SI} along the tangent, denoted by $\tau^{H_1}(x)$, $\tau^{H_2}(x)$ and $\omega_{SI}^{H_1}(x)$, $\omega_{SI}^{H_2}(x)$. Hence for a given value of $x \in (x_1, x_2)$ we can determine two points of the set H: $(\tau^{H_1}(x), \omega_{SI}^{H_1}(x))$ and $(\tau^{H_2}(x), \omega_{SI}^{H_2}(x))$. Thus the set H can be given as a union of two curves that are parametrised by $x \in (x_1, x_2)$. In Figure 6 the set H is shown for different values α_{SS}. We can see that as the value of α_{SS} decreases the interval (x_1, x_2) shrinks and below a critical value of α_{SS} it disappears, hence then H is the empty set.

Solving the ODE system (5)-(8) numerically one can see that if the parameter pair (τ, ω_{SI}) is inside the Hopf bifurcation curve then there is a stable limit cycle, see Figure 9D. If the parameter pair (τ, ω_{SI}) is outside the Hopf bifurcation curve then there is

no limit cycle. Thus along the Hopf bifurcation curve supercritical Hopf bifurcation occurs at the endemic steady state. We note that at the disease-free steady state there is no Hopf bifurcation, namely according to Proposition 3 the second condition of the Routh-Hurwitz criterion cannot be violated and it is known that the condition of the Hopf bifurcation is equivalent to the last but one Routh-Hurwitz condition [3, 2].
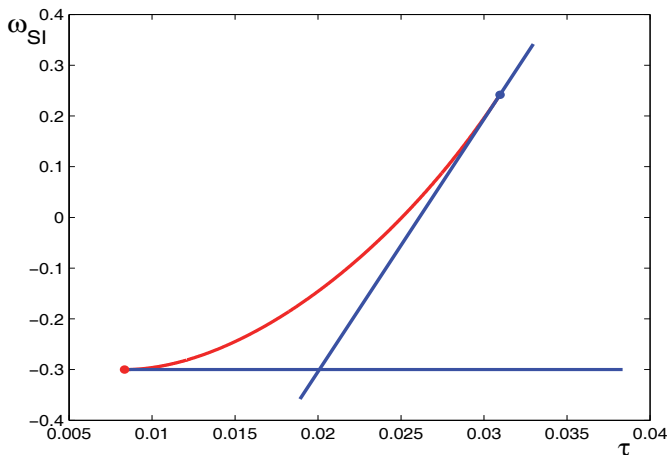

Figure 1. The D-curve and its tangents at the endpoints for $N = 100, n = 5, \alpha_{SI} = 0.3, \alpha_{SS} = 0.1, \alpha_{II} = 0, \omega_{SS} = 0.3, \omega_{II} = 0, \gamma = 1$. The blue endpoint belongs to $x = 0$ and the red one belongs to $x = N$.
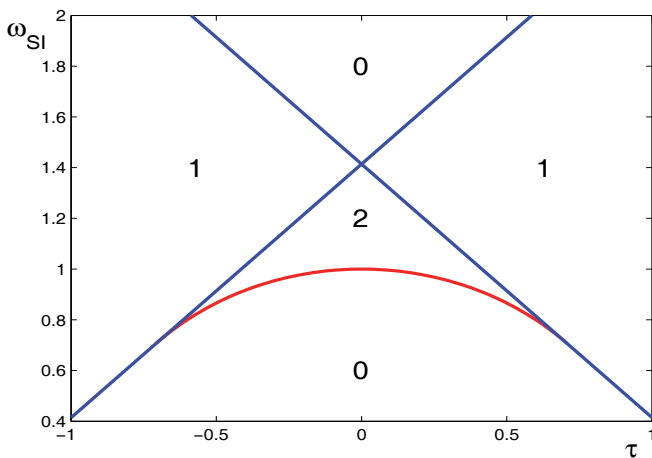
Figure 2. The number of tangents that can be drawn from different points to the given convex arc.
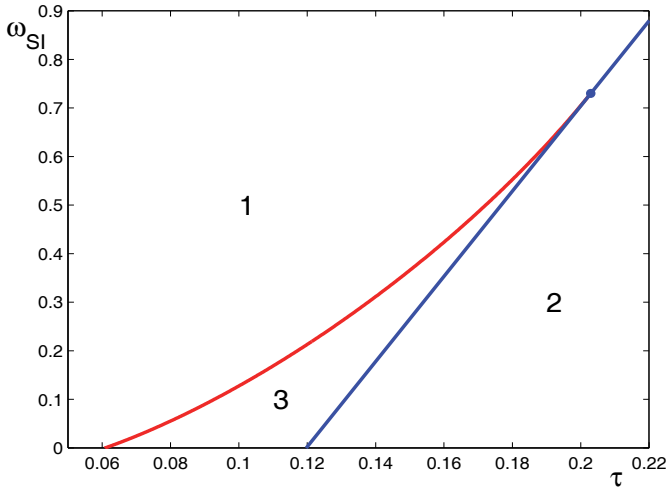
Figure 3. The D-curve and its tangent at the endpoint belonging to $x = 0$ divide the parameter plane into three domains according to the number of tangents. The numbers in the regions denote the number of steady states of system (5)-(8). The value of the parameters are $N = 100, n = 5, \alpha_{SI} = 0.05, \alpha_{SS} = 0.01, \alpha_{II} = 0, \omega_{SS} = 0.2, \omega_{II} = 0, \gamma = 1$.
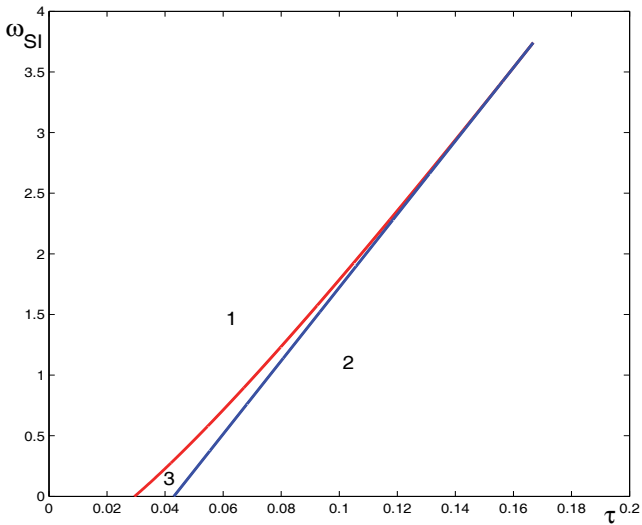

Figure 4. The D-curve in the case when $\alpha_{II} \neq 0 \neq \omega_{II}$. The D-curve and its tangent at the endpoint belonging to $x = 0$ divide the parameter plane into three domains according to the number of tangents. The numbers in the regions denote the number of steady states of system (5)-(8). The value of the parameters are $N = 100, n = 5, \alpha_{SI} = 0.3, \alpha_{SS} = 0.001, \alpha_{II} = 0.0001, \omega_{SS} = 0.3, \omega_{II} = 0.09, \gamma = 1$.
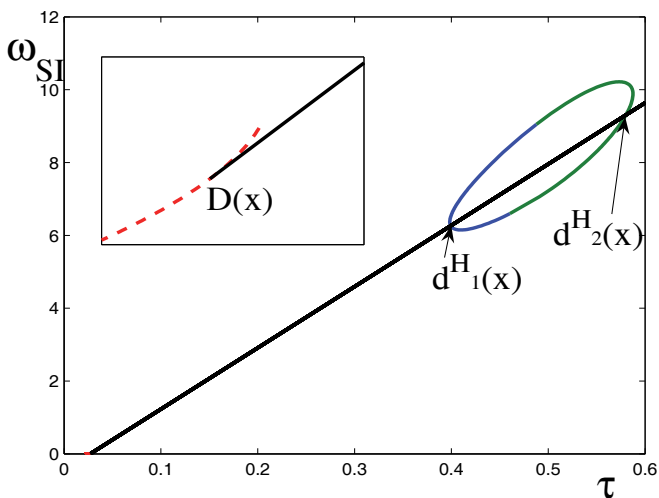
Figure 5. The method for finding the points of the Hopf bifurcation curve. Let us start from a point $D(x)$ of the D-curve, that is the dotted red line in the insert. The insert is the enlargement of the bottom part of the Figure containing the D-curve (shown in red) and a part of the tangent line (black). Draw a tangent to the D-curve at the point $D(x)$ and introduce a distant measure d. The tangent line can intersect the Hopf bifurcation curve (closed curve shown in green and blue) at two points, the distant of which from $D(x)$ are denoted by $d^{H_1}(x)$ and $d^{H_2}(x)$. The intersection point with the blue part of the Hopf curve is $d^{H_1}(x)$, and the intersection point with the green part is $d^{H_2}(x)$. The values of the parameters are $N = 100, n = 5, \alpha_{SI} = 0.007, \alpha_{II} = 0, \omega_{SS} = 0.007, \omega_{II} = 0, \gamma = 1$.
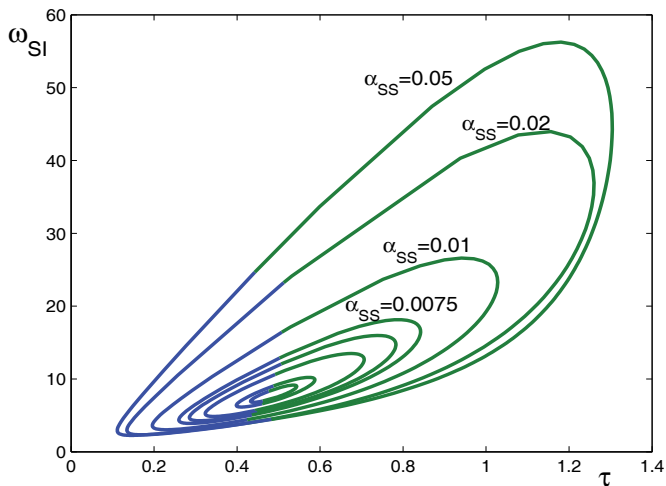

Figure 6. The set H for different values of α_{SS}. The values of the remaining parameters are $N = 100, n = 5, \alpha_{SI} = 0.007, \alpha_{II} = 0, \omega_{SS} = 0.007, \omega_{II} = 0, \gamma = 1$. The blue curves correspond to $(\tau^{H_1}(x), \omega_{SI}^{H_1}(x))$, the green ones correspond to $(\tau^{H_2}(x), \omega_{SI}^{H_2}(x))$. The small curves belong to $\alpha_{SS} = 0.007, 0.0065, 0.006, 0.0059$.
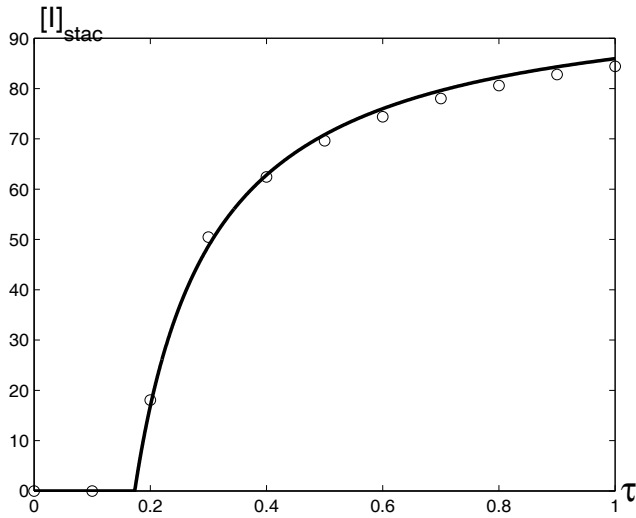
Figure 7. The comparison of simulation results (circles) and the steady state value of I obtained from the ODE (continuous line) for different values of τ. The values of the other parameters are $N = 100, n = 3, \alpha_{SI} = \alpha_{SS} = \alpha_{II} = 0.04, \omega_{SI} = \omega_{SS} = \omega_{II} = 0.5, \gamma = 1$.
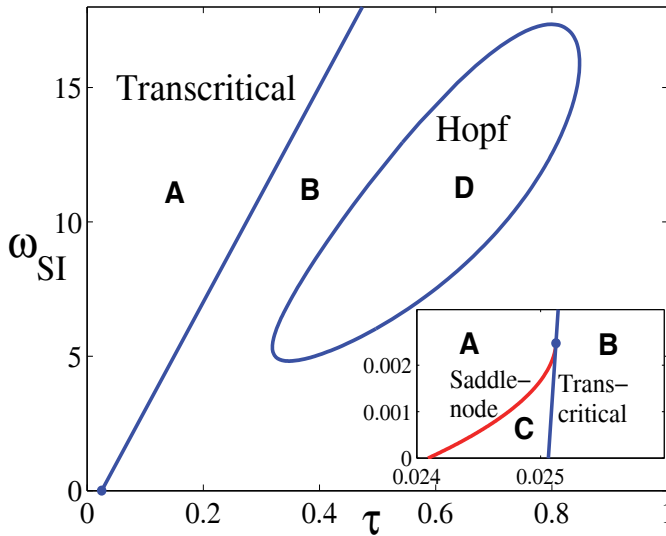

Figure 8. The three bifurcation curves for $N = 100, n = 10, \alpha_{SI} = 0.005, \alpha_{SS} = 0.004, \alpha_{II} = 0, \omega_{SS} = 0.005, \omega_{II} = 0, \gamma = 1$.
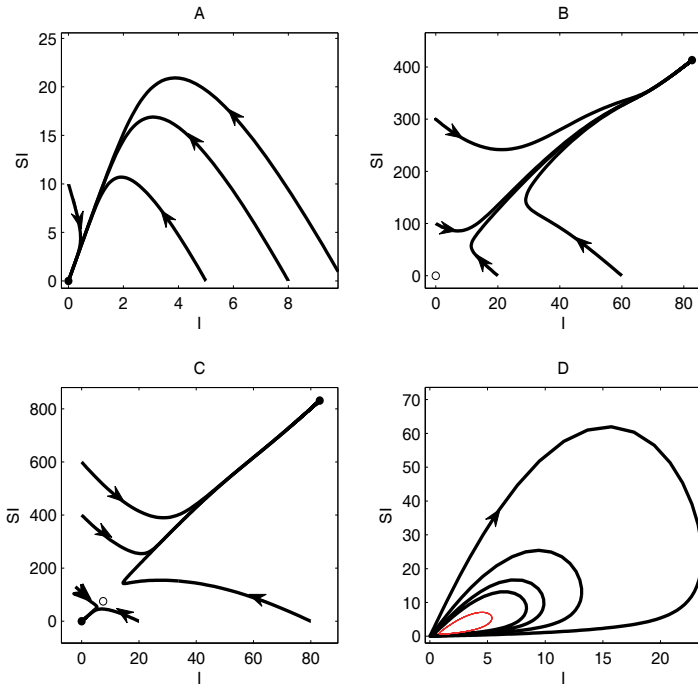
Figure 9. The (I, SI) projection of the phase portraits belonging to (τ, ω_{SI}) parameter pairs in the four different regions of the bifurcation diagram shown in Figure 8. The values of the other parameters are $N = 100, n = 10, \alpha_{SI} = 0.005, \alpha_{SS} = 0.004, \alpha_{II} = 0, \omega_{SS} = 0.005, \omega_{II} = 0, \gamma = 1$.

4. Discussion

We investigated the propagation of an SIS type epidemic on a network where edges of different type (i.e. SI, II and SS) can be activated or deleted according to a simple rule. This and similar phenomena can be modeled either via direct individual-based stochastic simulations or some type of ODE-based model that aims to approximate the evolution of average behaviour seen in simulations. The question of the agreement between the two different approaches is important and, for the model proposed here, we studied it in a previous paper [15]. Here we only illustrate the good agreement for the transcritical bifurcation, where the expected number of infected nodes is plotted as a function of τ, see Figure 6. The figure shows that the transcritical bifurcation, from both simulation and the ODE model, is observed at approximately $\tau = 0.17$, where the disease-free steady state looses its stability and an endemic steady state arises. In this paper our aim was to investigate the bifurcations of the ODE model in detail, and in

the case when the *II* links cannot be neither deleted nor created, we proved that the system can have at most three steady states one of them being the trivial, disease-free steady state. Three different kinds of bifurcation may occur. First, we have shown that the transcritical bifurcation of the trivial steady state leads to an endemic (non-trivial) steady state. We have also shown that saddle-node bifurcation takes place for a certain combination of parameter values, and the parametric representation method was used to give explicit analytic formulas yielding the saddle-node bifurcation curve in the plane of two important parameters, namely τ, the infection rate and ω_{SI} the rate of deletion of infecting, *SI* edges. Using this bifurcation curve, the exact number of steady states were determined in Theorem 1. Finally, we have derived formulas for the Hopf bifurcation curve in the above mentioned (τ, ω_{SI}) parameter plane, and have determined a parameter region where a stable periodic orbit exists. The full bifurcation picture is shown in Figure 8, and the phase portraits corresponding to the four regions in the bifurcation diagram are shown in Figure 9. Provided that the agreement between simulation and ODE models hold, the ODE-model provides a fast and reliable method that can quickly shed light on possible model behaviours. This is especially important when dealing with models with a large number of parameters where simulations alone are time consuming and it is difficult to explore possible model outcomes fully.

REFERENCES

[1] G. CSÖRGŐ, P. L. SIMON, *Bifurcations in the differential equation model of a chemical reaction*, Annales Univ. Sci. Budapest., **53** (2010), 45–57.

[2] H. FARKAS, P. L. SIMON, *Use of the parametric representation method in revealing the root structure and Hopf bifurcation*, J. Math. Chem., **9** (1992), 323–339.

[3] W. GOVAERTS, J. GUCKENHEIMER, A. KHIBNIK, *Defining functions for multiple Hopf bifurcations*, SIAM J. Numer. Anal., **34** (1997), 1269–1288.

[4] T. GROSS, C. J. DLIMA DOMMAR, B. BLASIUS, *Epidemic dynamics on an adaptive network*, Phys. Rev. Lett., **96** 208701, 2006.

[5] T. GROSS, B. BLASIUS, *Adaptive coevolutionary networks: a review*, J. Roy. Soc. Interface, **5** (2008), 259–271.

[6] T. HOUSE, M. J. KEELING, *Insights from unifying modern approximations to infections on networks*, J. Roy. Soc. Interface, **8** (2010), 67–73.

[7] M. J. KEELING, *The effects of local spatial structure on epidemiological invasions*, Proc. R. Soc. Lond. B, **266** (1999), 859–867.

[8] B. NAGY, *Analysis of the Biological Clock of Neurospora*, J. Comp. Appl. Math., **226** (2009), 298–305.

[9] S. RISAU-GUSMAN, D. H. ZANETTE, *Contact switching as a control startegy for epidemic outbreaks*, J. Theor. Biol., **257** (2009), 52–60.

[10] J. SARAMÄKI, K. KASKI, *Modelling development of epidemics with dynamic small-world networks*, J. Theor. Biol., **234** (2005), 413–421.

[11] L. B. SHAW, I. B. SCHWARTZ, *Fluctuating epidemics on adaptive networks*, Phys. Rev. E, **77**, 066101, 2008.

[12] P. L. SIMON, H. FARKAS, M. WITTMANN, *Constructing global bifurcation diagrams by the parametric representation method*, J. Comp. Appl. Math., **108** (1999), 157–176.

[13] P. L. SIMON, E. HILD, H. FARKAS, *Relationships between the discriminant curve and other bifurcation diagrams*, J. Math. Chem., **29** (2001), 245–265.

[14] M. TAYLOR, P. L. SIMON, D. M. GREEN, T. HOUSE, I. Z. KISS, *From Markovian to pairwise epidemic models and the performance of moment closure approximations*, J. Math. Biol., DOI: 10.1007/s00285-011-0443-3.

[15] I. Z. KISS, L. BERTHOUZE, T. J. TAYLOR, P. L. SIMON, *Modelling approaches for simple dynamic networks and applications to disease transmission models*, submitted to Proc. R. Soc. A.

András Szabó
Institute of Mathematics
Eötvös Loránd University
Budapest
Hungary
e-mail: szaboa@cs.elte.hu

Péter L. Simon
Institute of Mathematics
Eötvös Loránd University
Budapest
Hungary
e-mail: simonp@cs.elte.hu

Istvan Z. Kiss
School of Mathematical and Physical Sciences
Department of Mathematics, University of Sussex
Falmer, Brighton BN1 9RF, UK
e-mail: i.z.kiss@sussex.ac.uk

Differential Equations & Applications
www.ele-math.com
dea@ele-math.com